Optical and Topological Characterization of Hexagonal DNA Origami Nanotags

Congzhou Chen
Peking University https://orcid.org/0000-0001-8425-3416
Jin Xu
Peking University
Xiaolong Shi (xlshi@gzhu.edu.cn)
Guangzhou University

Research

Keywords: DNA origami, atomic force microscopy, uorescence labelling, nano-ruler

Posted Date: October 1st, 2020

DOI: https://doi.org/10.21203/rs.3.rs-73565/v1

Version of Record: A version of this preprint was published at IEEE Transactions on NanoBioscience on January 1st, 2021. See the published version at https://doi.org/10.1109/TNB.2021.3095157.

RESEARCH

Optical and Topological Characterization of Hexagonal DNA Origami Nanotags

Congzhou Chen[1], Jin Xu[1] and Xiaolong Shi[2*]

*Correspondence:
xlshi@gzhu.edu.cn
[2]Institute of Computing Science & Technology, Guangzhou University., DüXihuan Road 230, 510006 Guangzhou, China
Full list of author information is available at the end of the article
†Equal contributor

Abstract

Background:DNA origami can be applied as a "ruler" for nanoscale calibration or super-resolution fluorescence microscopy with an ideal structure for defining fluorophore arrangement, allowing the distance between fluorophores to be precisely controlled at the nanometer scale. DNA origami can also be used as a nanotag with arbitrary programmable shapes.
Results: We formed a hexagonal origami structure embedded with three different fluorescent dyes on the surface. The distance between each fluorescent block was 120 nm, which is below the diffraction limit of light, allowing for its application as a nano-ruler for super-resolution fluorescence microscopy. The outside edge of the hexagonal structure was redesigned to form three different substructures as topological labels. Atomic and scanning force microscopy demonstrated consistency of the nanoscale distance between morphological and fluorescent labels.
Conclusion: We assembled the hexagonal origami platform and confirmed the fluorescent and topological labels, this fluorophore-embedded hexagonal origami platform can be used as a dual nano-ruler for both optical and topological calibration.

Keywords: DNA origami; atomic force microscopy; fluorescence labelling; nano-ruler

INTRODUCTION

DNA origami has various applications, including DNA computing, nanoarchitecture, and drug design. [1–9] Single-DNA origami is formed by a long circular scaffold strand with the help of hundreds of staple strands, [10] each of which is known in advance and has a unique position in the final assembled structure. The size of a single origami is determined by the length of its scaffold strand, which generally has an area in the nanometer scale. DNA origami also provides an excellent platform for super-resolution fluorescent microscopy owing to advantages of optical calibration, which allows for precise docking of the fluorophores at predesigned positions. Therefore, DNA origami facilitates studying the characteristics of fluorescent dyes at different distances. [11–16]

To date, DNA origami has been used to develop several types of two-dimensional fluorescent nanotags, including cylindrical or rectangular structures. [14, 16] Such compact origami structures are proven to be robust and stable with fluorophores embedded at target locations. Owing to the precise distance control of fluorophores, the energy transfer between different fluorescent dyes can be calculated, [17] which allows for selection of the most suitable fluorescent dye under different conditions of

interest. [16] Further, fluorophore-embedded origami structures were demonstrated to serve as an ideal calibration ruler for a variety of super-resolution microscopy applications, including stimulated emission depletion microscopy (STED), direct stochastic optical reconstruction microscopy, or confocal microscopy. [18–20] With further development of this technology, even a single biomolecule (<5 nm) can be identified such as DNA-paint. [21–23] Recently, a fluorophores-embedded origami ruler has been commercialized and is becoming widely applied (Gattaquant, Braunschweig, Germany).

As a single origami structure is in the nanometer size scale, several origamis need to be assembled into a larger shape to enable fluorescent microscopy at different scales, including the microscale, for various purposes. For example, a cross-shaped origami was utilized to construct finite arrays, and different fluorescent dyes were deposited onto the substrate. [24] In addition, polyhedra self-assembled three-dimensional origami structures were formed using DNA origami tripods with fluorophores attached onto each vertex, and the 1–60 MD super DNA gridiron was characterized using three-dimensional DNA-paint. [25]

All of these previously developed structures were designed as fluorescent nanotags for calibration. However, the origami itself was neglected in these previous designs. As DNA origami can be formed in arbitrary shapes, topological tags are possible. [26] The lack of consideration of the topological characteristics of the origami has hampered its broader application in versatile fields such as for genotyping and shape detection. [27] Moreover, an atomic force microscope (AFM) has much higher resolution than a fluorescent microscope in detecting topological features. In this study, we designed a hexagonal DNA origami platform with both spectral and topological features by docking three types of fluorescent dyes onto the surface, and three types of substructures were programmed and attached at the edge of the platform. We used optical and topological characterizations to demonstrate the utility of this new platform as a dual tag in nano-calibration.

EXPERIMENT

Design Strategy. The hexagonal origami was assembled using six triangular origami tiles, which were previously reported by Paul Rothemund.10 We modified the triangular origami by loosening the outside edge (Fig.1) , resulting in a tadpole-like shape: a triangular origami with a loosened tail (Fig. 2b).

The connection strategy followed the originally reported method; the connecting (inner) edges of the triangle were sorted as extended and truncated edges (corresponding staple strands were extend or truncated for conncetion). By changing the positions of each connecting part, the triangular origami was divided into three groups (Supplementary Fig. S1). The outside edge was loosened (the scaffold was left single stranded), leaving a region of 845 nucleotides for further topological design.

The DNA strands used in this study were purchased from Sangon Biotech (Shanghai, China) and HAP-purified. The single-strand M13mp18 scaffold was purchased from New England BioLabs (Beijing, China). Staple and scaffold strands were mixed at a 1:10 ratio, the mixed solution was diluted in 1× TAE buffer with 12.5 Mg2+, and then annealing was performed by reducing the temperature from 95°C to 4°C for 13 h.

After forming the single triangular origami, the samples were purified using ultrafilter tubes (Millipore Ultra-100K, Millipore Shanghai, China) at 9000 rpm for 5 min. The concentration of the three tubes was measured on a spectrophotometer (Step Thermo Fisher NanoDrop One, Thermo Fisher Scientific, Waltham, MA, USA) at an ultraviolet wavelength (260 nm) for DNA. The single triangular origamis were then maintained at 4°C until further processing.

The three groups of triangular origamis were assembled into a hexagonal platform while precisely controlling the ratio of the three groups at 1:1:1. Assembly was performed with incubation at 45°C for 2 days. The assembled hexagonal samples were then electrophoresed for further purification. The gel harboring the hexagonal platform was cut for purification, and the refined hexagonal samples were used as nanotags (Fig. 2c). The yield of the assembled hexagon was calculated using ImageJ (National Institutes of Health, Bethesda, MD, USA).

AFM Characterization. We used a Bruker Multimode 8 serial AFM (Bruker Corporation, Karlsruhe, Germany) for optical characterization, operating at the "ScanAsyst in Fluid" mode with Scan in Fluid tips. First, 5μl of the hexagonal sample was dripped onto a fresh mica surface and left for 5 min to allow the sample to completely absorb onto the mica surface, followed by the addition of 20μl 1× TAE buffer. The sample was then placed on the piezoelectric ceramic stage for scanning. We set the AFM to "ScanAsyst in Fluid" mode using Scan in Fluid tips. The approaching surface set point was 0.075 V; after approaching the mica surface, the AFM functioned at automated set points in auto scan mode with a scan rate of 2 Hz per second.

Super-Resolution Characterization. Two illuminations are required with a STED system: one for excitation and the other for loss of light. In this study, we used the Leica STED 3X serial system for super-resolution microscopy to acquire fluorescent images. This is a high-resolution microscope based on the confocal microscopy system; its x/y plane resolution is $\leq$50 nm and the z-space resolution is$\leq$130 nm.

We chose three dyes for analysis with this platform: Alex 488, Cy3, and Cy5. Alex 488 is a green fluorescent dye with an excitation spectrum at the 488-nm laser line. Cy3 is an orange dye with an excitation wavelength at 600 nm, and Cy5 is a red dye with an excitation wavelength at 700 nm. All three dyes are all highly fluorescence-sensitive and photostable, and are further resistant to light bleaching. These characteristics facilitate identification of the dyes on the platform through a STED microscope.

The hexagonal origami platform was attached to a coverslip surface via a sandwich linking strategy using bovine serum albumin (BSA)-biotin, streptavidin, and a BSA-biotin bridge. All of the triangle origamis were functionalized with biotin anchors at the back of their surfaces. We set eight docking positions for each triangular origami, and six staple strands at the bule points were extended 12 nt with BSA-biotin modification (Supplementary Fig. S2).

Clean coverslips were soaked in a BSA-biotin solution (0.1 mg/ml) and left for 1 h to allow the biotin to completely absorb onto the surface. The coverslips were then washed with phosphate-buffered saline (PBS; 11 mM Mg2+), followed by soaking in a streptavidin solution (50 nM) for 1 h, and air drying.

The samples were embedded onto the prepared and dried coverslips; a 5μl sample was uniformly pipetted onto the surface and dried at room temperature in a dark environment. Note that it is important to carefully store these samples while avoiding light.

The sample was placed onto the stage of the Leica TCS Sp8 STED 3X microscope and an appropriate field of view was selected under the bright field. The loading settings were excitation at 491 nm and 592 nm STED wavelengths for Alexa 488, 561-nm laser for Cy3, and 670-nm laser for Cy5. The laser wavelengths were chosen so as to cover the excitation peak spectrum of each dye. To prevent cross-coloring of the three fluorescent dyes, we used one laser at a time for detection of each dye. The intensity of the STED laser was set to its maximum power to obtain the best resolution ratio.

RESULTS AND DISCUSSION

Design and Assembly. As shown in Fig. 2c, our assembly strategy resulted in various subunits, including dual-, triple, quadra-, and penta-assemblies. This reflects inefficient connections due to the increasing difficulty in connections with a larger platform. Even when we maintained the sample at 45°C for 2 days, the yield of the hexagon was quite low at 21.4% (Supplementary Figure S3).

Super-Resolution Fluorescent Tag. STED is the first method that was applied to overcome the diffraction barrier of light. [28] In STED microscopy, reduction in the effective fluorescent luminescence area is achieved by stimulated emission effects.

We designed six docking sites at the outer edge of the triangle origami, including one of the three dyes: Alex 488 embedded on a single triangle origami for group one, Cy3 on group two, and Cy5 on group three. The blue dots in Fig. 3 indicate the docking positions for each fluorophore.

After forming the single triangle origami, a 20-times volume of fluorescent staple strands was added to each corresponding group and annealed at 45°C for 6 h, followed by ultrafiltration purification as described for forming the hexagonal platform. After annealing, the samples were purified through gel electrophoresis (Fig. S3). Representative super-resolution microscope images are shown in Figure 4.

Figure 4a–c show STED images of the tricolor-labeled platforms. The three colors docked separately, and the distance of each fluorophore was 160–240 nm. Although this spectrum distance is longer than the spatial distance of the fluorophores (120 nm), it is still considered to be acceptable since light diffraction remains to affect the super-resolution system.

To further verify the ability of this platform, we constructed a bicolored tag combining Cy5 and Alexa 488 (Figure 4d–f). The cyclic halo with two identical fluorophores shows the dual color-labeled origami platform. The two fluorophores Cy5 (red) and Alexa 488 (green) have the furthest spectrum distance among the three dyes. The two dyes were circularly arranged on the platform by rearranging the linking strands for the two triangular origami groups. The distance between the two colors shown in Figure 4d and 4e was around 200 nm, considering the light diffraction as the distance feature of two separate dyes.

In addition, we verified the monochromatic origami platform, displaying clear orange halos for Cy3 (Fig. 4g), red halos for Cy5 (Fig. 4h), and green halos for Alexa 488 (Fig. 4i), demonstrating attachment of the dyes to the platform.

Topological Labeling. As mentioned above, the outside edge of the triangular tile was loosened. We programmed three different topological labels for the platform: a triangular shape, rectangular shape, and striped shape. Figure 5 shows a schematic of each design.

In the topological labeling experiment, the three different substructures were assigned to each group, which were annealed, purified separately, and mixed at a 1:1:1 ratio. The last step involved refining the topological labels by refining the hexagonal origami from gel brick. The AFM image of the refined sample is shown in Figure 6 and Supplementary Fig. S4.

As shown in Fig. 6, some subunits remained in the sample, which indicated structures that were not successfully purified. This could lead to a negative effect on the calibration. Nonetheless, in the STED images, all of the platforms appeared as circular halos with different colors docked separately, and the hexagonal platform could still be distinguished from the subunits in the AFM images. Additionally, purification with gel electrophoresis demonstrated that most of the structures were a hexagonal platform. In a larger scan image, the topological figures appear as six dots around the platform.

Notably, there were some distortions in the substructures. The striped-shaped label was folded into a "V" shape because of the instability of this structure and the triangular substructure was distorted as a circle. These distortions were the result of theorematics randomness, and the instability of substructures that were assembled by a few staple strands (<500 nucleotides).

CONCLUSION

In this study, we combined fluorescent nanotags with topological labels to form a dual-nanotag platform. The fluorescent characteristics were detected using a STED super-resolution microscope and the topological labels were identified using AFM.

This strategy offers a dual method for calibrating nanoscale samples. Recently, dual in situ calibration has emerged as a research hotspot for the design of nanorulers, [29,30] and many researchers and companies are actively engaged in manufacturing in situ microscopes. Although our experiment was not flawless, most notably owing to the remnant subunits indicating imperfect purification, we believe this strategy offers the possibility for realizing spectrum- and topological-based nanotag calibration. Further studies and improvements can be implemented on this basis.

Competing interests
The authors declare that they have no competing interests.

Ethics approval and consent to participate
Not applicable.

Acknowledgements
Not applicable.

Consent for publication
Written informed consent for publication was obtained from all participants.

Availability of data and material
All data generated or analyzed during this study are included in this article.

Author's contributions

The manuscript was written through contributions of all authors. All authors have given approval to the final version of the manuscript.

Funding

This work was supported by the National Key R & D Program of China (Grant No. 2019YFA0706402), National Natural Science Foundation of China (61632002, 61872399, 61872166, 61672264 and 61772376) and Pilot Project (19-ZLXD-04-12-03-200-02).

Author details

[1]Key Laboratory of High Confidence Software Technologies of Ministry of Education, Institute of Software, School of Electronics Engineering and Computer Science, Peking University, Yiheyuan Road, 430079 Beijing, China. [2]Institute of Computing Science & Technology, Guangzhou University., DüXihuan Road 230, 510006 Guangzhou, China.

References

1. Woods, D., Doty, D., Myhrvold, C., Hui, J., Zhou, F., Yin, P., Winfree, E.: Diverse and robust molecular algorithms using reprogrammable dna self-assembly. Nature **567**(7748), 366–372 (2019)
2. Shi, X., Lu, W., Wang, Z., Pan, L., Cui, G., Xu, J., LaBean, T.H.: Programmable dna tile self-assembly using a hierarchical sub-tile strategy. Nanotechnology **25**(7), 075602 (2014)
3. Shi, X., Chen, C., Li, X., Song, T., Chen, Z., Zhang, Z., Wang, Y.: Size-controllable dna nanoribbons assembled from three types of reusable brick single-strand dna tiles. Soft matter **11**(43), 8484–8492 (2015)
4. Chen, C., Xu, J., Shi, X.: Adjusting linking strands to form size-controllable dna origami rings. IEEE Transactions on NanoBioscience **19**(2), 167–172 (2020)
5. Xu, J.: Probe machine. IEEE transactions on neural networks and learning systems **27**(7), 1405–1416 (2016)
6. Shi, X., Wu, X., Song, T., Li, X.: Construction of dna nanotubes with controllable diameters and patterns using hierarchical dna sub-tiles. Nanoscale **8**(31), 14785–14792 (2016)
7. Chao, J., Wang, J., Wang, F., Ouyang, X., Kopperger, E., Liu, H., Li, Q., Shi, J., Wang, L., Hu, J., *et al.*: Solving mazes with single-molecule dna navigators. Nature Materials **18**(3), 273–279 (2019)
8. Kwon, P.S., Ren, S., Kwon, S.-J., Kizer, M.E., Kuo, L., Xie, M., Zhu, D., Zhou, F., Zhang, F., Kim, D., *et al.*: Designer dna architecture offers precise and multivalent spatial pattern-recognition for viral sensing and inhibition. Nature chemistry **12**(1), 26–35 (2020)
9. Li, S., Jiang, Q., Liu, S., Zhang, Y., Tian, Y., Song, C., Wang, J., Zou, Y., Anderson, G.J., Han, J.-Y., *et al.*: A dna nanorobot functions as a cancer therapeutic in response to a molecular trigger in vivo. Nature biotechnology **36**(3), 258 (2018)
10. Rothemund, P.W.: Folding dna to create nanoscale shapes and patterns. Nature **440**(7082), 297–302 (2006)
11. Schnitzbauer, J., Strauss, M.T., Schlichthaerle, T., Schueder, F., Jungmann, R.: Super-resolution microscopy with dna-paint. Nature protocols **12**(6), 1198 (2017)
12. Raab, M., Jusuk, I., Molle, J., Buhr, E., Bodermann, B., Bergmann, D., Bosse, H., Tinnefeld, P.: Using dna origami nanorulers as traceable distance measurement standards and nanoscopic benchmark structures. Scientific reports **8**(1), 1–11 (2018)
13. Strauss, M.T., Schueder, F., Haas, D., Nickels, P.C., Jungmann, R.: Quantifying absolute addressability in dna origami with molecular resolution. Nature communications **9**(1), 1–7 (2018)
14. Schmied, J.J., Gietl, A., Holzmeister, P., Forthmann, C., Steinhauer, C., Dammeyer, T., Tinnefeld, P.: Fluorescence and super-resolution standards based on dna origami. Nature methods **9**(12), 1133–1134 (2012)
15. Graugnard, E., Hughes, W.L., Jungmann, R., Kostiainen, M.A., Linko, V.: Nanometrology and super-resolution imaging with dna. MRS bulletin **42**(12), 951 (2017)
16. Beater, S., Holzmeister, P., Pibiri, E., Lalkens, B., Tinnefeld, P.: Choosing dyes for cw-sted nanoscopy using self-assembled nanorulers. Physical Chemistry Chemical Physics **16**(15), 6990–6996 (2014)
17. Ozhalıcı-Unal, H., Armitage, B.A.: Fluorescent dna nanotags based on a self-assembled dna tetrahedron. ACS nano **3**(2), 425–433 (2009)
18. Schmied, J.J., Raab, M., Forthmann, C., Pibiri, E., Wünsch, B., Dammeyer, T., Tinnefeld, P.: Dna origami–based standards for quantitative fluorescence microscopy. Nature protocols **9**(6), 1367–1391 (2014)
19. Dai, M., Jungmann, R., Yin, P.: Optical imaging of individual biomolecules in densely packed clusters. Nature nanotechnology **11**(9), 798–807 (2016)
20. Johnson-Buck, A., Nangreave, J., Kim, D.-N., Bathe, M., Yan, H., Walter, N.G.: Super-resolution fingerprinting detects chemical reactions and idiosyncrasies of single dna pegboards. Nano letters **13**(2), 728–733 (2013)
21. Jungmann, R., Avendaño, M.S., Woehrstein, J.B., Dai, M., Shih, W.M., Yin, P.: Multiplexed 3d cellular super-resolution imaging with dna-paint and exchange-paint. Nature methods **11**(3), 313–318 (2014)
22. Raab, M., Schmied, J.J., Jusuk, I., Forthmann, C., Tinnefeld, P.: Fluorescence microscopy with 6 nm resolution on dna origami. ChemPhysChem **15**(12), 2431–2435 (2014)
23. Jungmann, R., Steinhauer, C., Scheible, M., Kuzyk, A., Tinnefeld, P., Simmel, F.C.: Single-molecule kinetics and super-resolution microscopy by fluorescence imaging of transient binding on dna origami. Nano letters **10**(11), 4756–4761 (2010)
24. Korpelainen, V., Linko, V., Seppä, J., Lassila, A., Kostiainen, M.A.: Dna origami structures as calibration standards for nanometrology. Measurement Science and Technology **28**(3), 034001 (2017)
25. Iinuma, R., Ke, Y., Jungmann, R., Schlichthaerle, T., Woehrstein, J.B., Yin, P.: Polyhedra self-assembled from dna tripods and characterized with 3d dna-paint. science **344**(6179), 65–69 (2014)
26. Ke, Y., Lindsay, S., Chang, Y., Liu, Y., Yan, H.: Self-assembled water-soluble nucleic acid probe tiles for label-free rna hybridization assays. Science **319**(5860), 180–183 (2008)
27. Zhang, H., Chao, J., Pan, D., Liu, H., Qiang, Y., Liu, K., Cui, C., Chen, J., Huang, Q., Hu, J., *et al.*: Dna origami-based shape ids for single-molecule nanomechanical genotyping. Nature communications **8**(1), 1–7 (2017)

28. Harke, B., Keller, J., Ullal, C.K., Westphal, V., Schönle, A., Hell, S.W.: Resolution scaling in sted microscopy. Optics express **16**(6), 4154–4162 (2008)
29. Reinhard, B.M., Siu, M., Agarwal, H., Alivisatos, A.P., Liphardt, J.: Calibration of dynamic molecular rulers based on plasmon coupling between gold nanoparticles. Nano letters **5**(11), 2246–2252 (2005)
30. Nadig, S., Lal, A.: In-situ calibration of mems inertial sensors for long-term reliability. In: 2018 IEEE International Reliability Physics Symposium (IRPS), pp. 3–8 (2018). IEEE

Figures

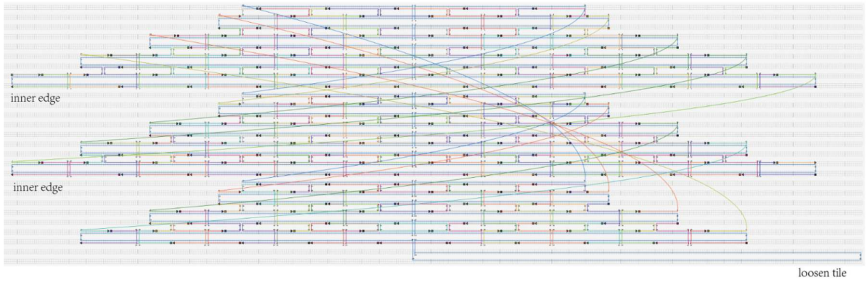

Figure 1 Triangular origami was designed by using caDNAno. The length of the edge is 120 nm. As a modification, we loosened the outside edge of the triangle. The two inner edges were used as the linking sites for assembly.

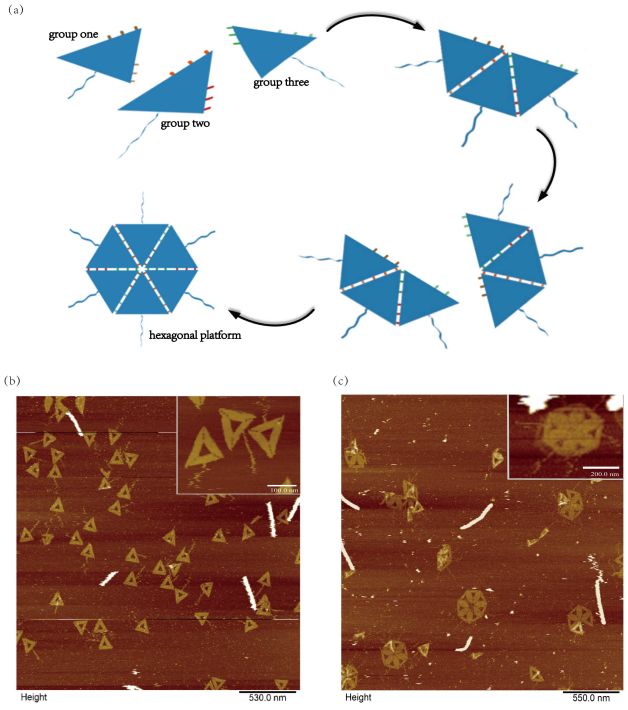

Figure 2 (a) Single triangular tiles assembled into a hexagonal platform; the outside edge is then available for design as a topological label. The triangular origamis were divided into three groups with unique linking strands. (b) Single triangle origami. (c) The hexagonal platform.

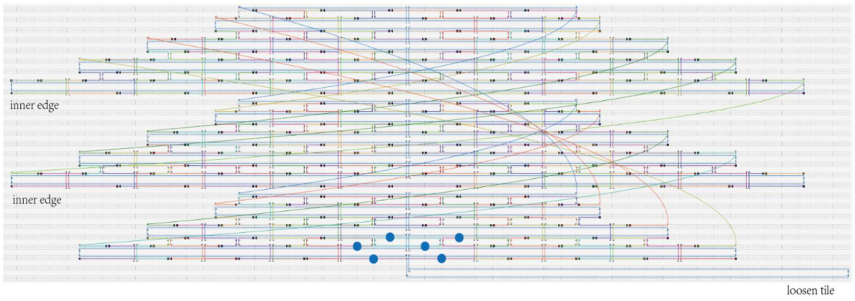

Figure 3 A single triangular origami with six docking strands at the brim of its outer edge. The loosened tile is 845 nucleotides long. The blue dots indicate the docking positions for fluorophores.

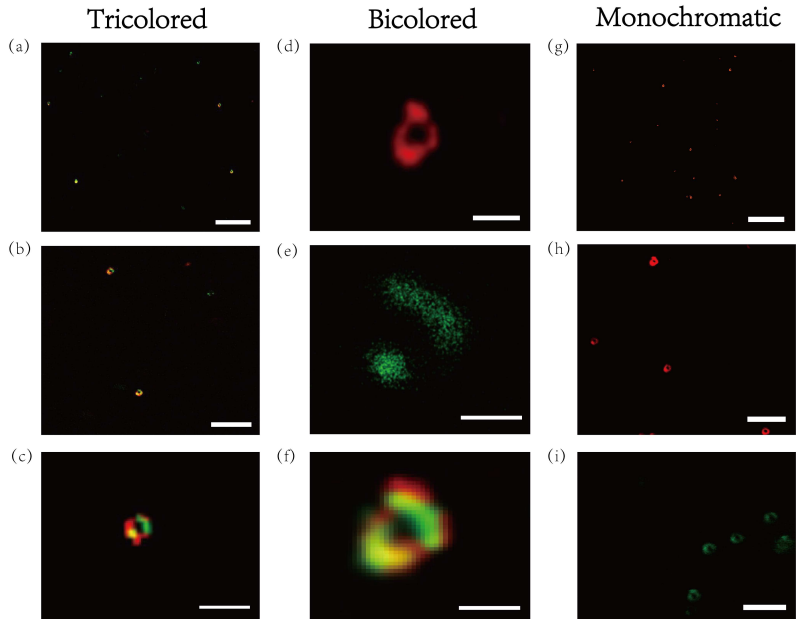

Figure 4 STED super-resolution microscope images. (a–c) Tricolored origami platform with Alex 488, Cy3, and Cy5 attached shown at three scales: (a) scale bar = 6 μm, (b) scale bar = 3 μm, (c) scale bar = 1 μm. (d) Cy5 attached (red); scale bar = 600 nm. (e) Alexa 488 attached (green); scale bar = 500 nm. (f) Bicolored origami platform combining Cy5 and Alexa 488; scale bar = 500 nm. (g–i) Monochromatic platforms with only (g) Cy3 (scale bar = 6 μm), (h) Cy5 (scale bar = 2 μm), and (i) Alexa 488 (scale bar = 2 μm) attached.

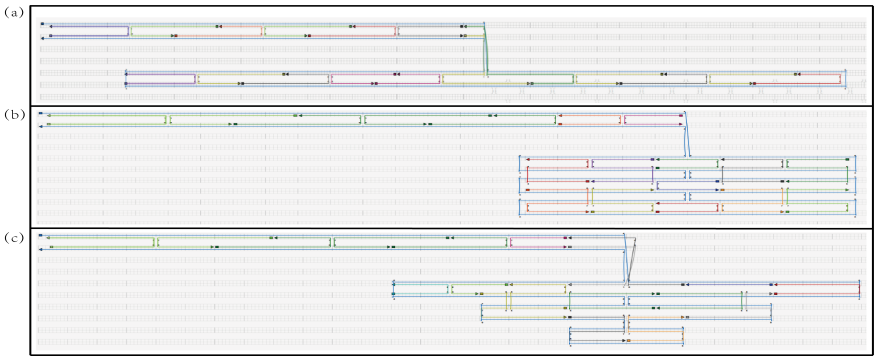

Figure 5 The three different topological labels. (a) Striped-shaped label. (b) Rectangular-shaped label. (c) Triangular-shaped label.

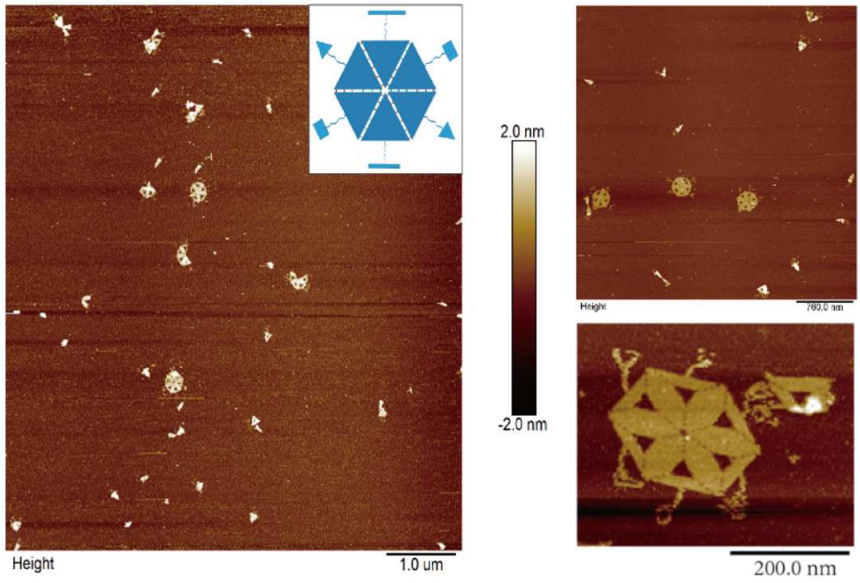

Figure 6 Topological labeling and design scheme. The three topological labels were identified, and different shapes were separately located. However, some subunits remained in the purified samples.

Figures

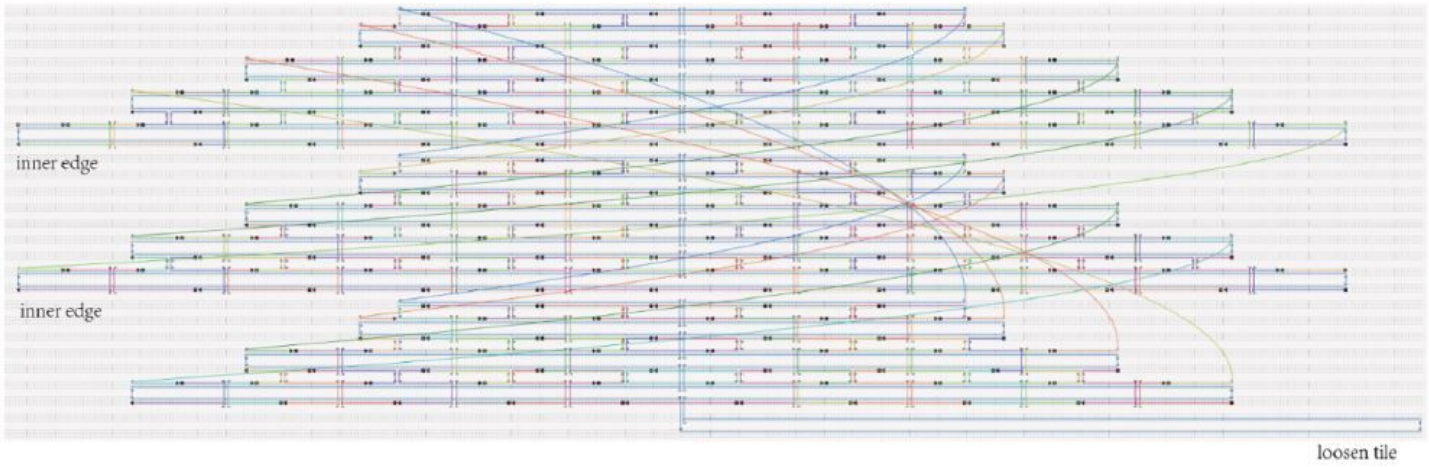

Figure 1

Triangular origami was designed by using caDNAno. The length of the edge is 120 nm. As a modification, we loosened the outside edge of the triangle. The two inner edges were used as the linking sites for assembly.

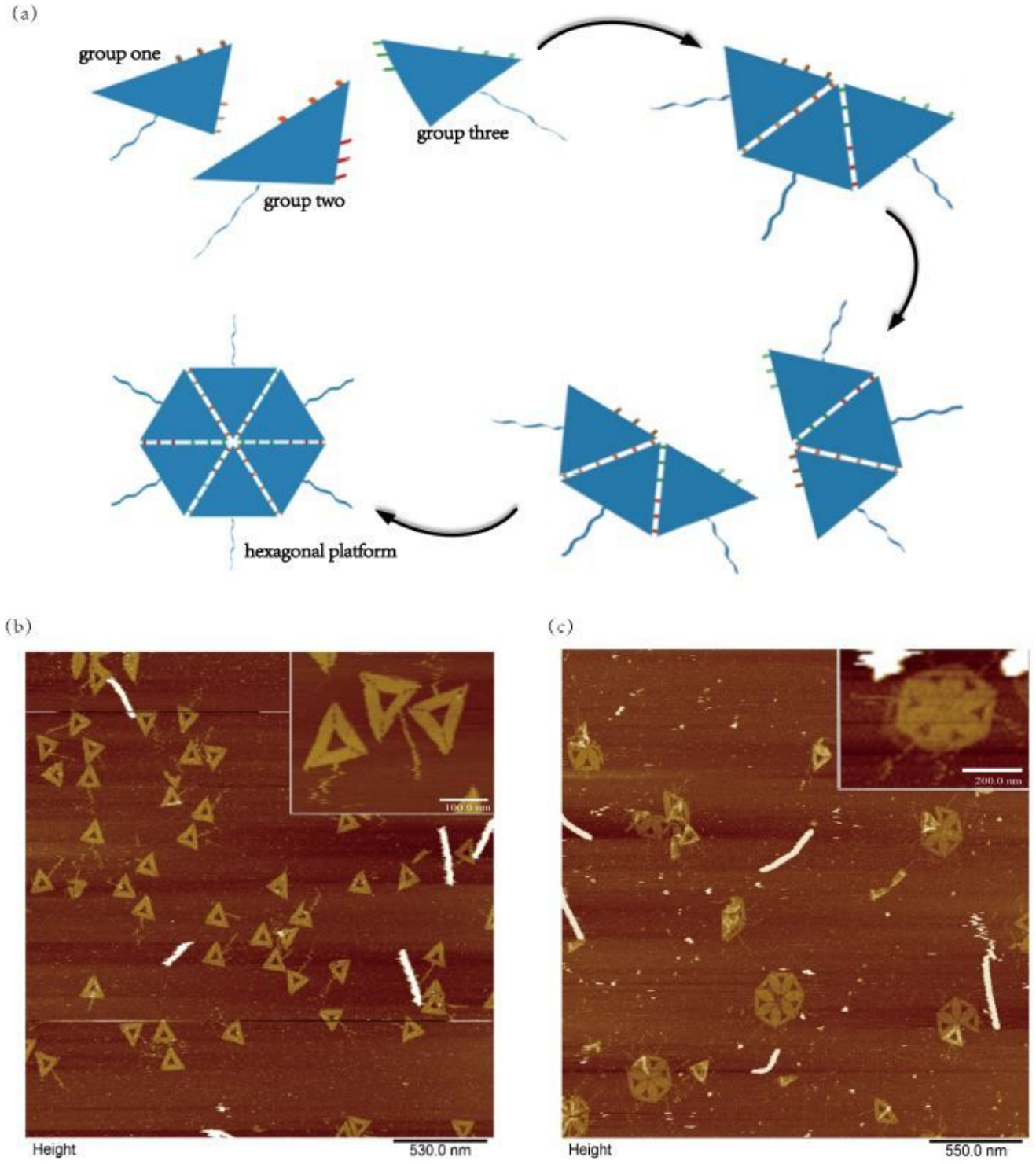

Figure 2

(a) Single triangular tiles assembled into a hexagonal platform; the outside edge is then available for design as a topological label. The triangular origamis were divided into three groups with unique linking strands. (b) Single triangle origami. (c) The hexagonal platform.

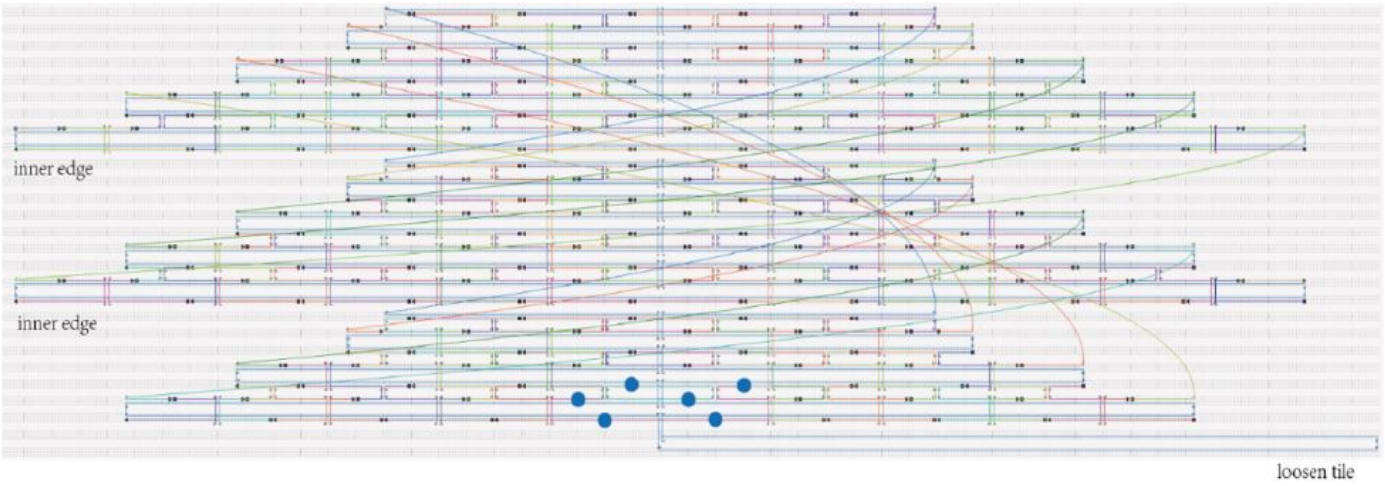

Figure 3

A single triangular origami with six docking strands at the brim of its outer edge. The loosened tile is 845 nucleotides long. The blue dots indicate the docking positions for fluorophores.

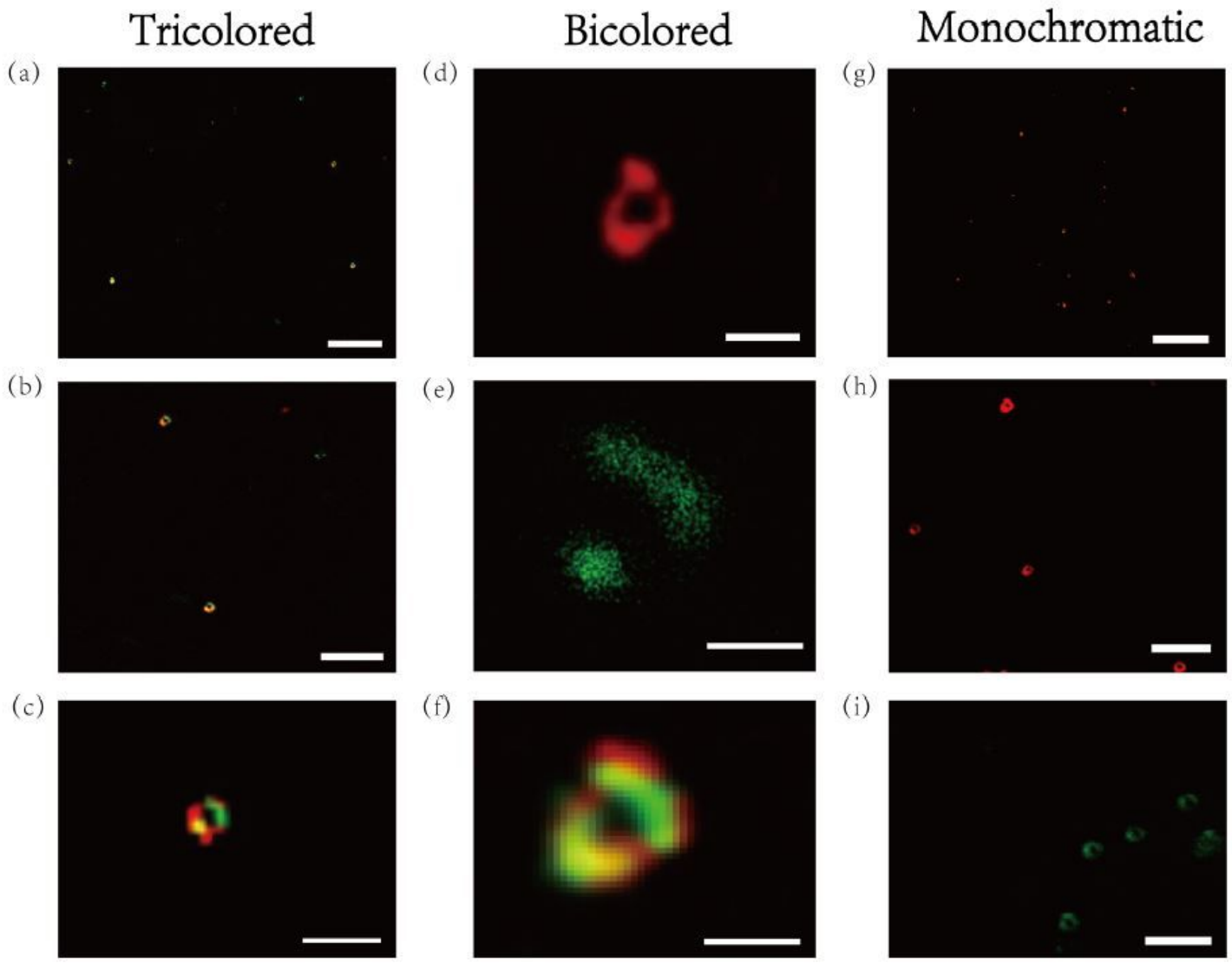

Figure 4

STED super-resolution microscope images. (a-c) Tricolored origami platform with Alex 488, Cy3, and Cy5 attached shown at three scales: (a) scale bar = 6 μm, (b) scale bar = 3 μm, (c) scale bar = 1 μm. (d) Cy5 attached (red); scale bar = 600 nm. (e) Alexa 488 attached (green); scale bar = 500 nm. (f) Bicolored origami platform combining Cy5 and Alexa 488; scale bar = 500 nm. (g{i) Monochromatic platforms with only (g) Cy3 (scale bar = 6 μm), (h) Cy5 (scale bar = 2 μm), and (i) Alexa 488 (scale bar = 2 μm) attached.

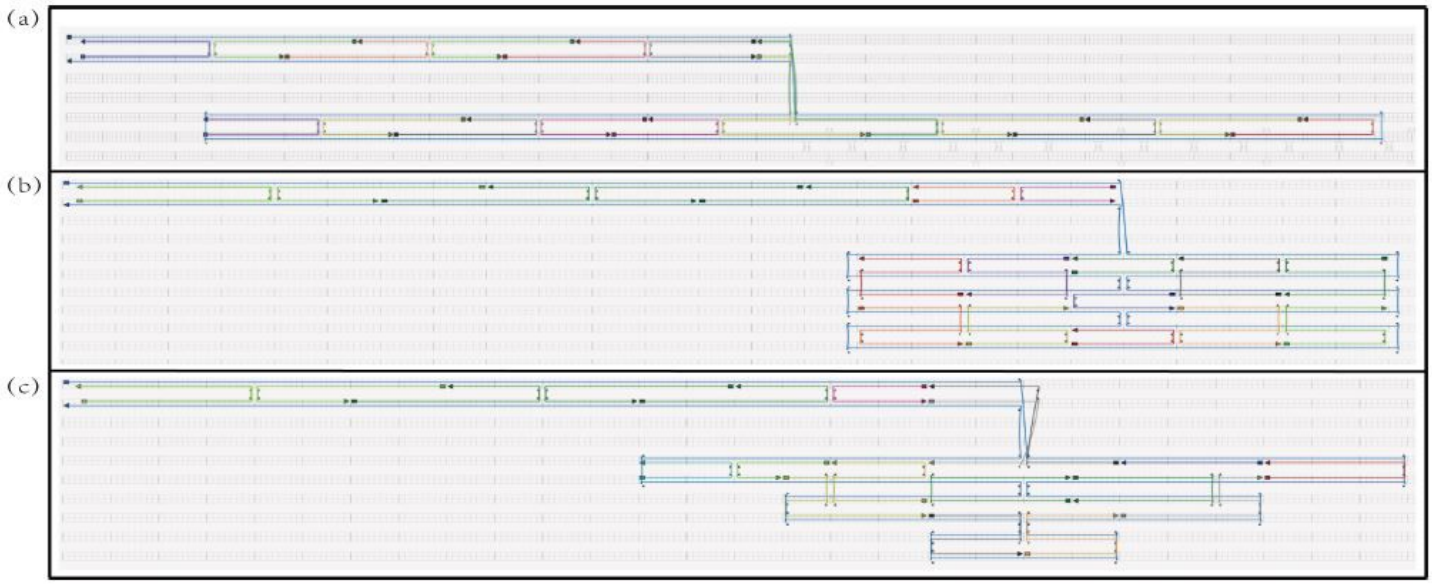

Figure 5

The three different topological labels. (a) Striped-shaped label. (b) Rectangular-shaped label. (c) Triangular-shaped label.

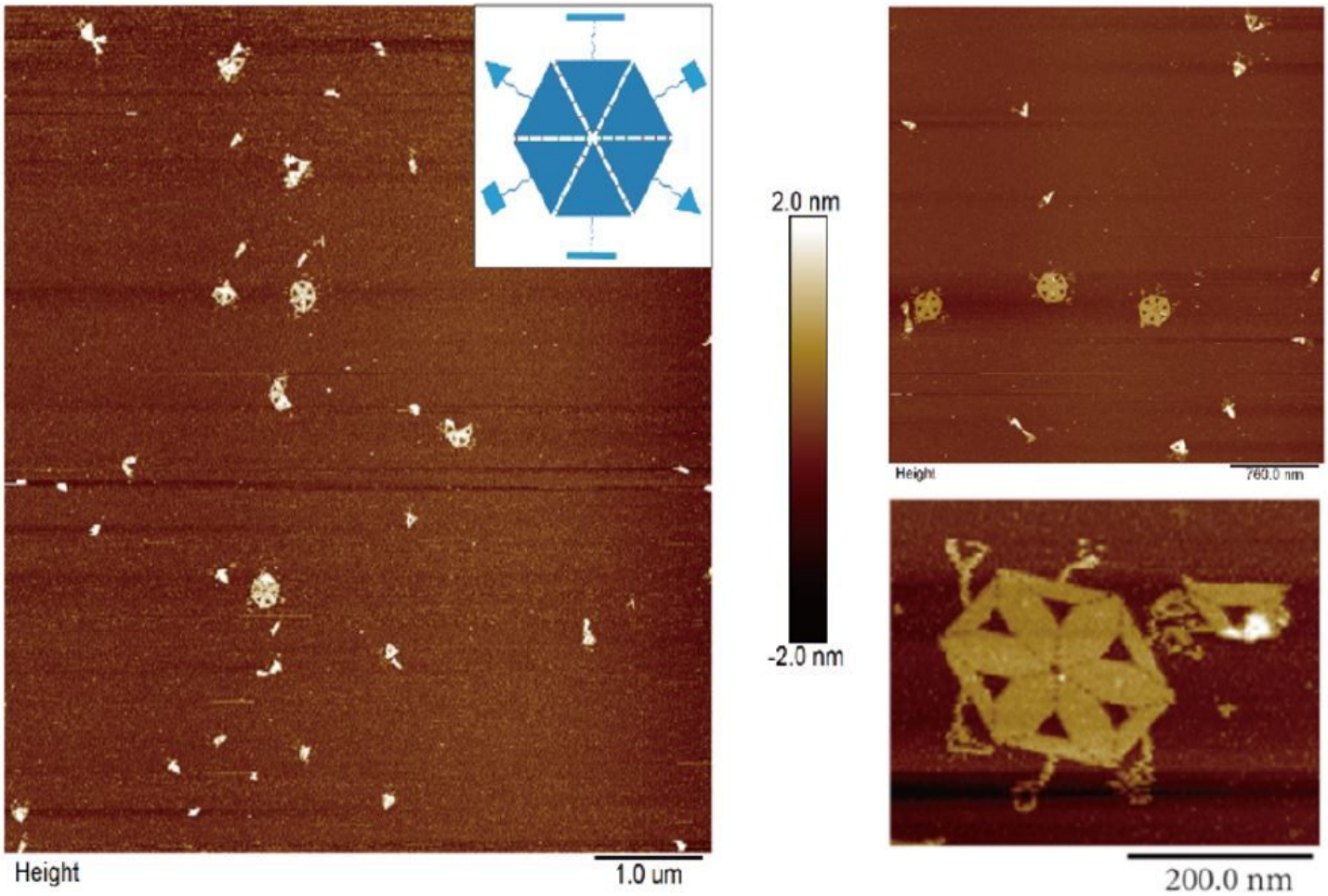

Figure 6

Topological labeling and design scheme. The three topological labels were identified, and different shapes were separately located. However, some subunits remained in the purified samples.

Supplementary Files

This is a list of supplementary files associated with this preprint. Click to download.

- Supplementary.pdf